

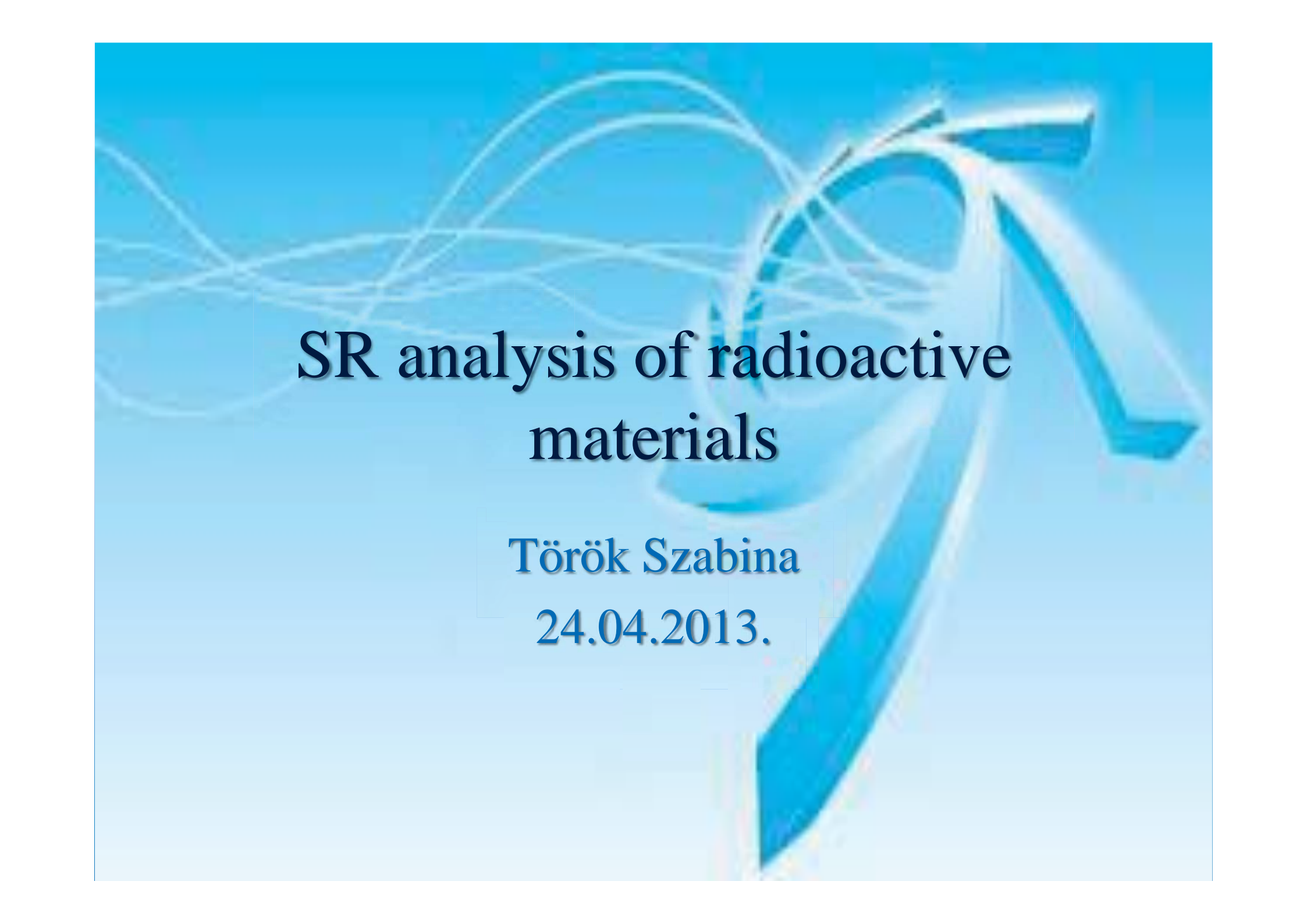
2454-4

**Joint ICTP-IAEA Workshop on Advanced Synchrotron Radiation Based X-ray
Spectrometry Techniques**

22 - 26 April 2013

SR analysis of radioactive materials

Török Szabina
*KFKI Atomic energy Research Institute
Budapest
Hungary*

The background is a solid light blue color. Overlaid on this are several white, thin, curved lines that sweep across the upper left portion of the slide. On the right side, there is a large, 3D, blue arrow pointing upwards and to the right, with a slight shadow effect.

SR analysis of radioactive materials

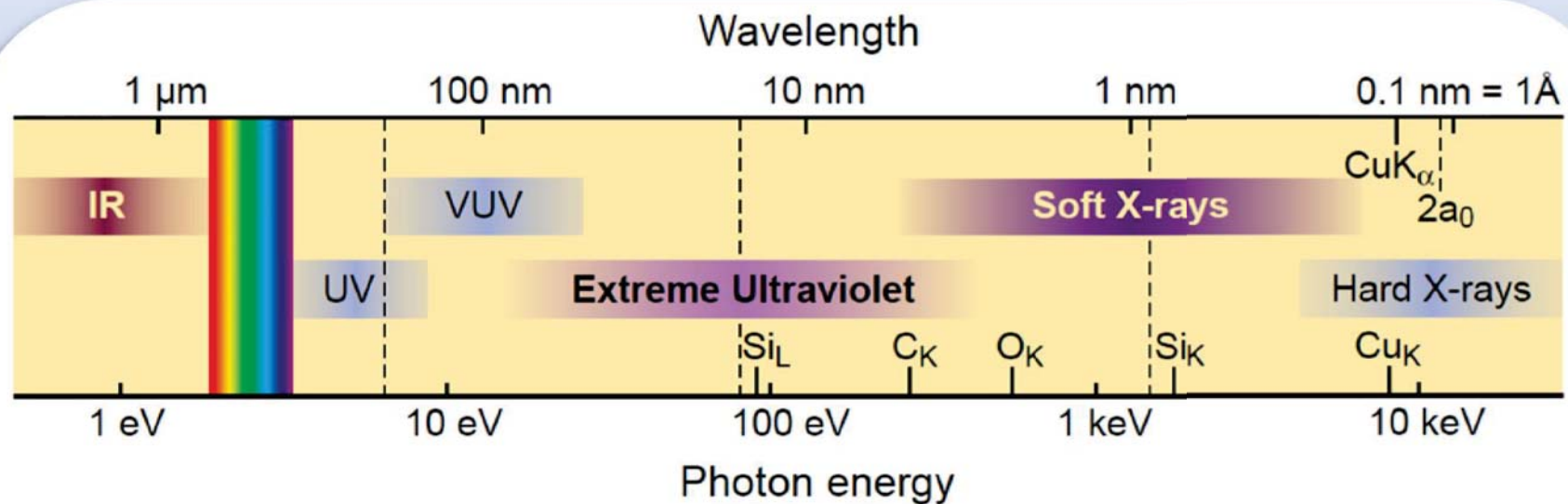
Török Szabina

24.04.2013.

Contents

- Radioactive problems where SR analysis provides significant contribution
- Micro-XRF and absorption spectroscopies of particles
- Sorption experiments with rocks from claystone formations, potential sites for underground high level radioactive waste
- Conclusions

The Short Wavelength Region of the Electromagnetic Spectrum



- See smaller features
- Write smaller patterns
- Elemental and chemical sensitivity

Scientists around the vacuum chamber of a 1947 General Electric synchrotron



SR was seen first at General Electric in 1947 in a different type of particle accelerator (synchrotron). It was first considered a nuisance because causing the particles to lose energy, but was then recognised in the 1960s as light with exceptional properties that overcame the shortcomings of X-ray tubes.

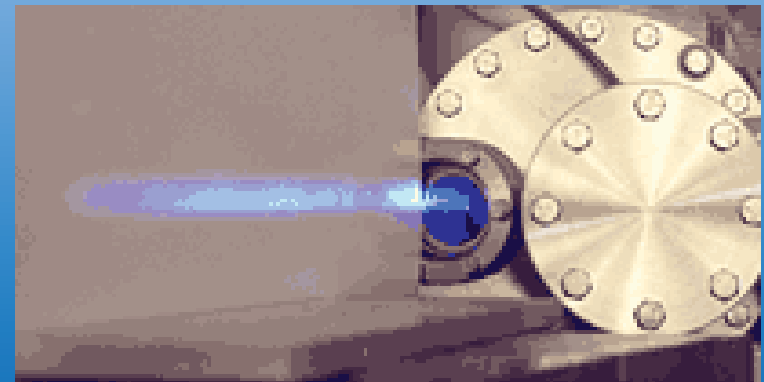
Initial construction of the National Synchrotron Light Source (NSLS)



1978



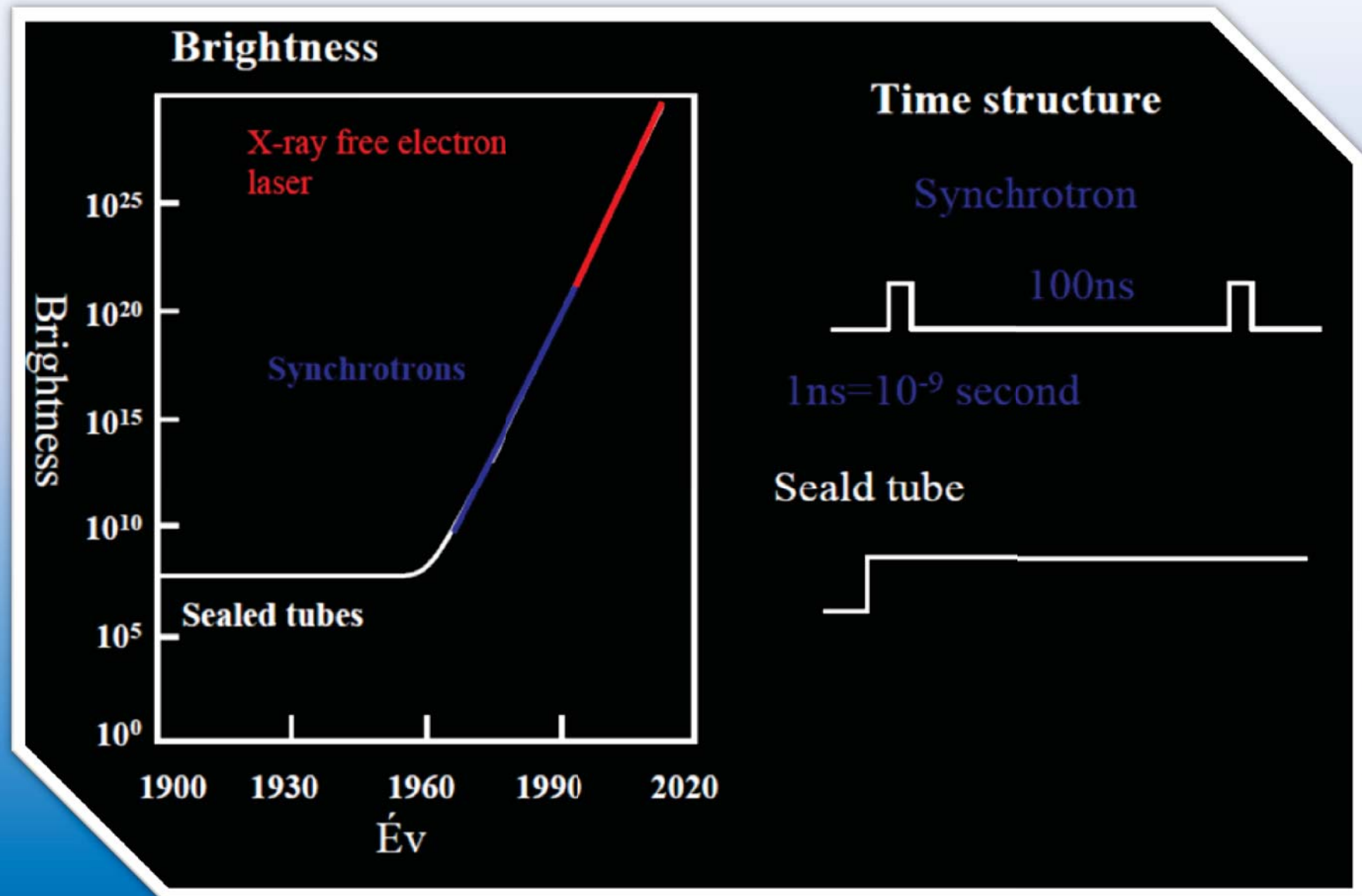
1982



Comaprison of sources

Synchrotrons		Scaled tubes
Temporal	pulsed (100 ns, 1 ns)	continouous
Spatial	collimated (mrad)	4π
Polarisation	linear (tunable)	unpolirased
Intensity	large	small
Brightness	large 10^{12} - 10^{18}	small 10^8

Characteristics of sources

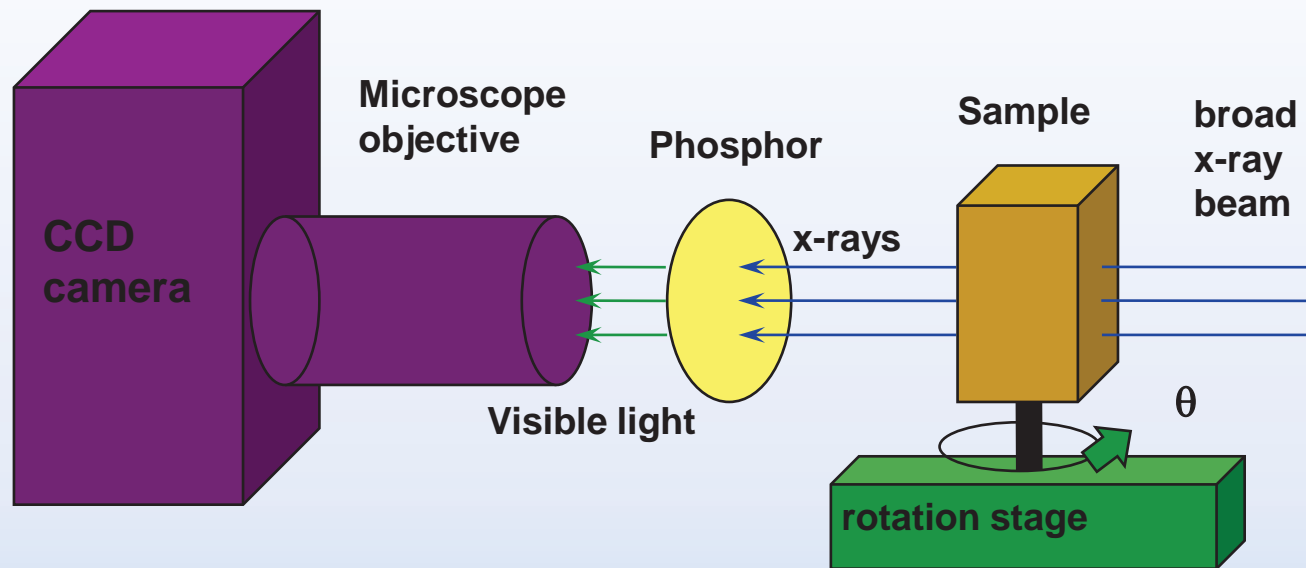


Most presently operational SR sources belong to the so-called second generation facilities. New third-generation storage rings obtain mono-energetic and high brilliance beams

SR has a major impact on microprobe-type methods like:

- micro-x-ray fluorescence (μ -XRF)
- x-ray absorption spectrometry (XAS, like XANES and EXAFS)
- total reflection x-ray fluorescence (TXRF)

X-ray Tomography: Overview

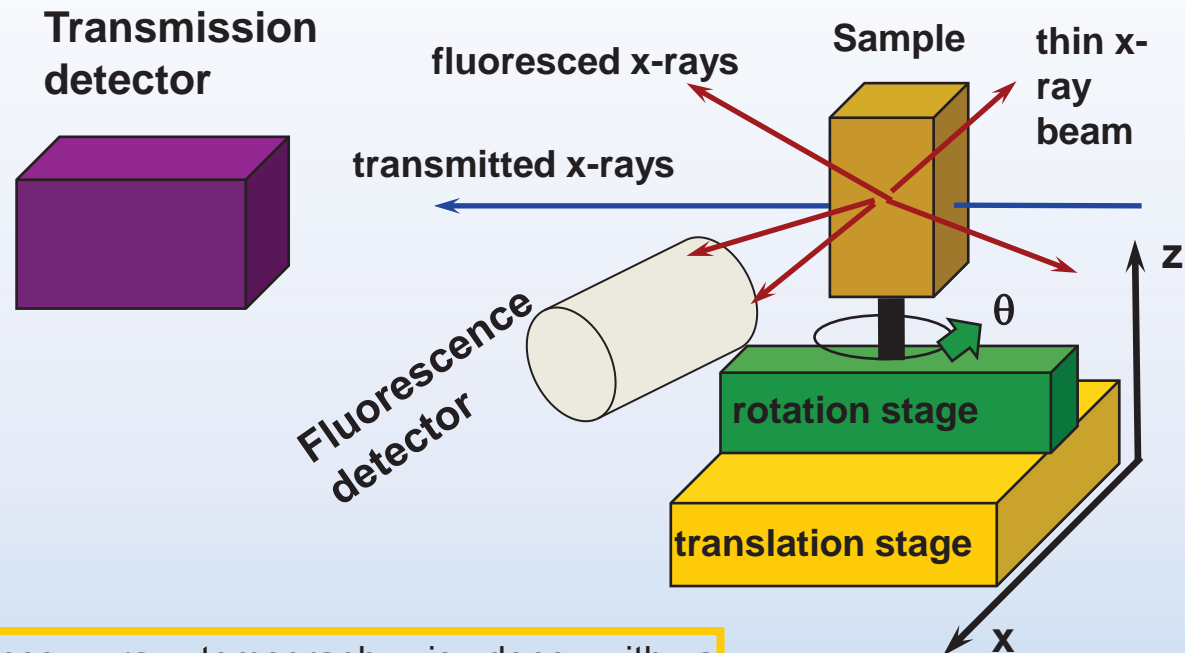


X-ray computed microtomography (CMT) gives 3D images of the x-ray attenuation coefficient within a sample.

At each angle, a 2D absorption image is collected. The angle is rotated around θ in 1° steps through 180° , and the 3D image is reconstructed with software.

Element-specific imaging can be done by acquiring tomograms with incident energies above and below an absorption edge.

X-ray Fluorescence Tomography

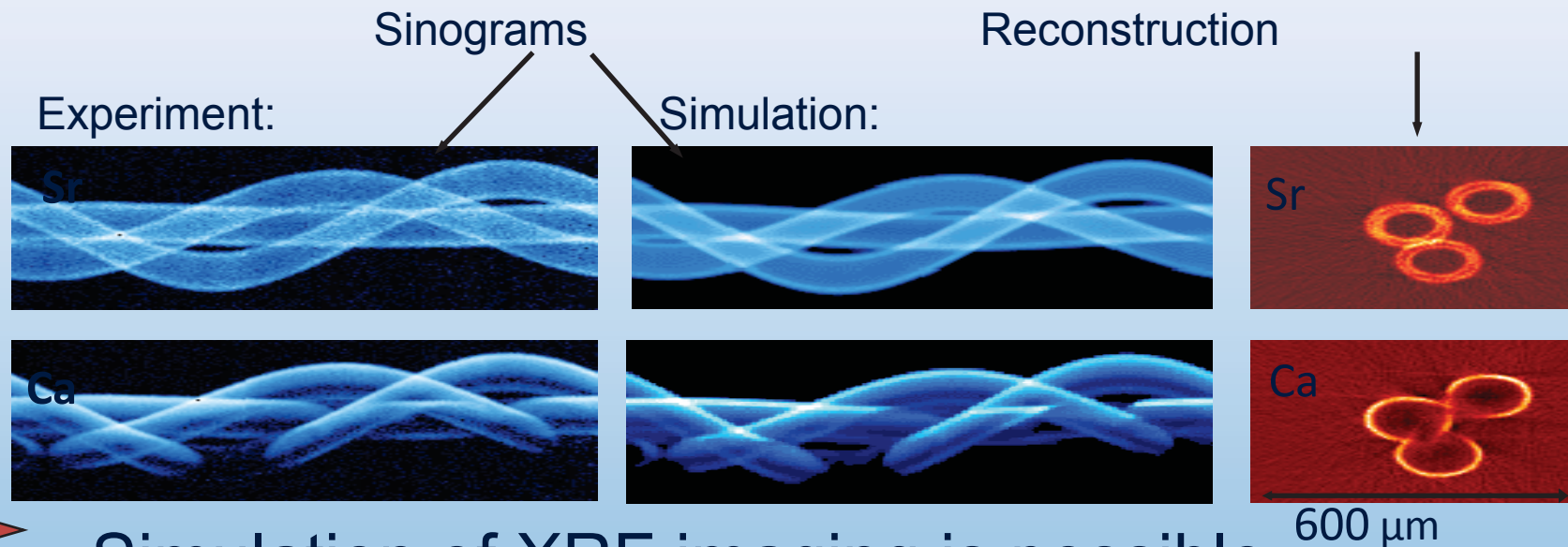
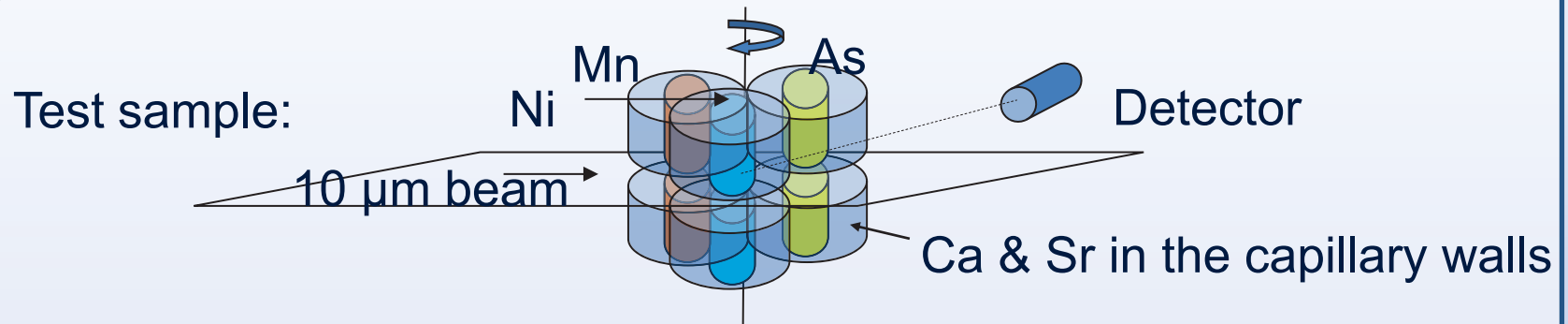


Fluorescence x-ray tomography is done with a **pencil-beam** scanned across the sample. The sample is rotated around θ and translated in x . Transmission x-rays can be measured as well to give an overall density tomograph.

- can collect multiple fluorescence lines,
- data collection is relatively slow,
- can be complicated by self-absorption.

G.F. Rust, and J. Weigelt *IEEE TRANSACTIONS ON NUCLEAR SCIENCE*, **75**, pp 14 (1998)
A. Simionovici, et al. in *Developments in X-Ray Tomography II*, SPIE Proceedings **3772**, 304-310 (1999)
A. Simionovici, et al, *Nuclear Instruments and Methods in Physics Research A*, **467-468**, pp 889-892 (2001)
C. G. Schroer, *Applied Physics Letters*, **79** (12), 1912-1914 (2001)

Simulation of heterogeneous materials: application to XRF tomography



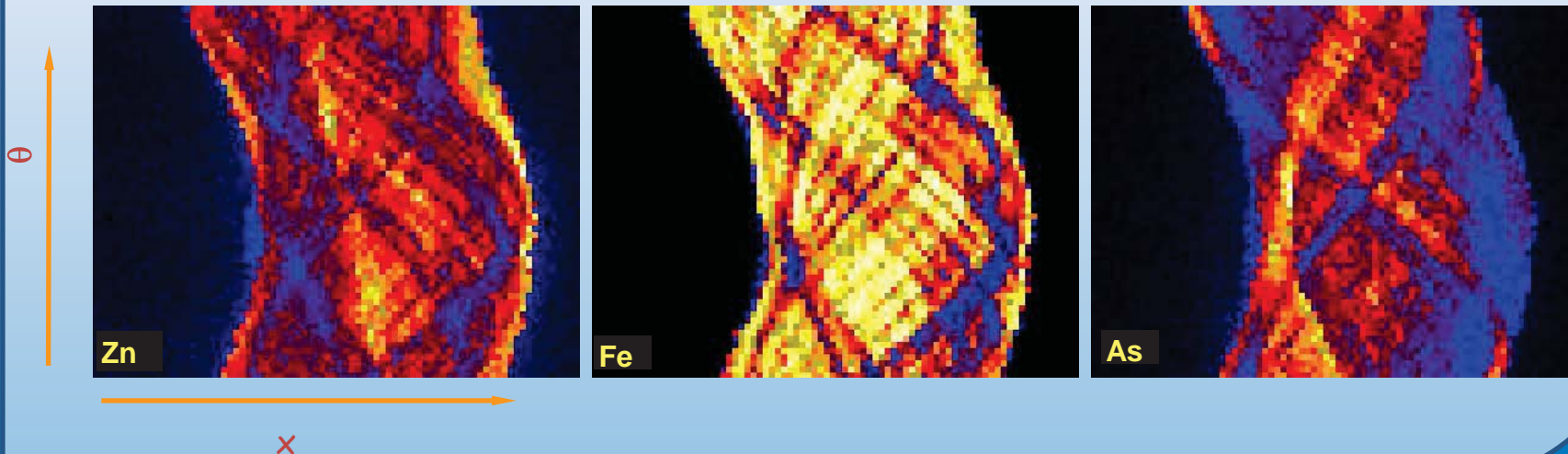
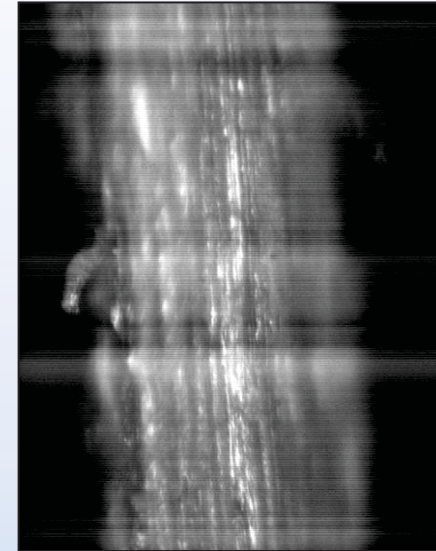
Simulation of XRF imaging is possible!

Courtesy: Laszlo Vincze, Univ. Antwerp

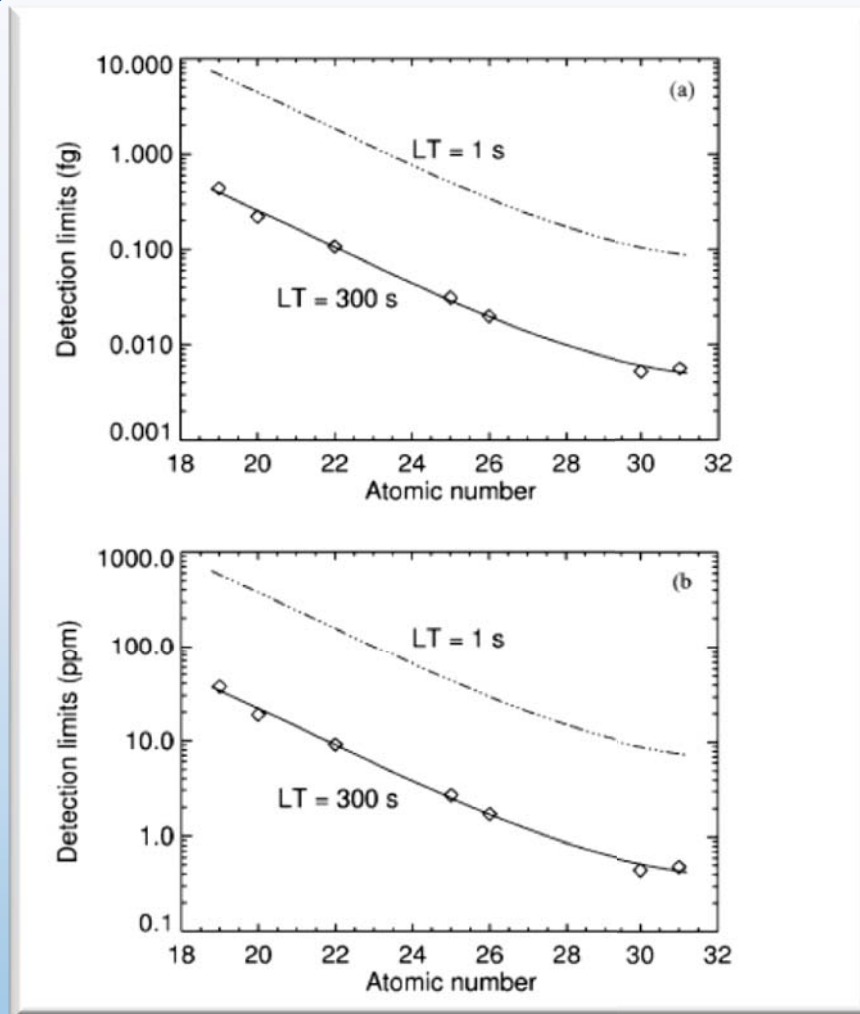
Fluorescence Tomography: Sinograms

The Raw fluorescence tomography data consists of elemental fluorescence (uncorrected for self-absorption) as a function of position and angle: a **sinogram**. This data is reconstructed as a virtual **slice** through the sample by a coordinate transformation of $(x, \theta) \rightarrow (x, y)$. The process can be repeated at different z positions to give three-dimensional information.

Fluorescence Sinograms for Zn, Fe, and As collected simultaneously for a section of contaminated root (photo, right): **x**: 300 μm in 5 μm steps **θ** : 180° in 3° steps



Absolute and relative XRF detection limits



300 and 1 s (dashed curve), respectively. The beam size used was 220 nm × 170 nm, 12.7 keV.

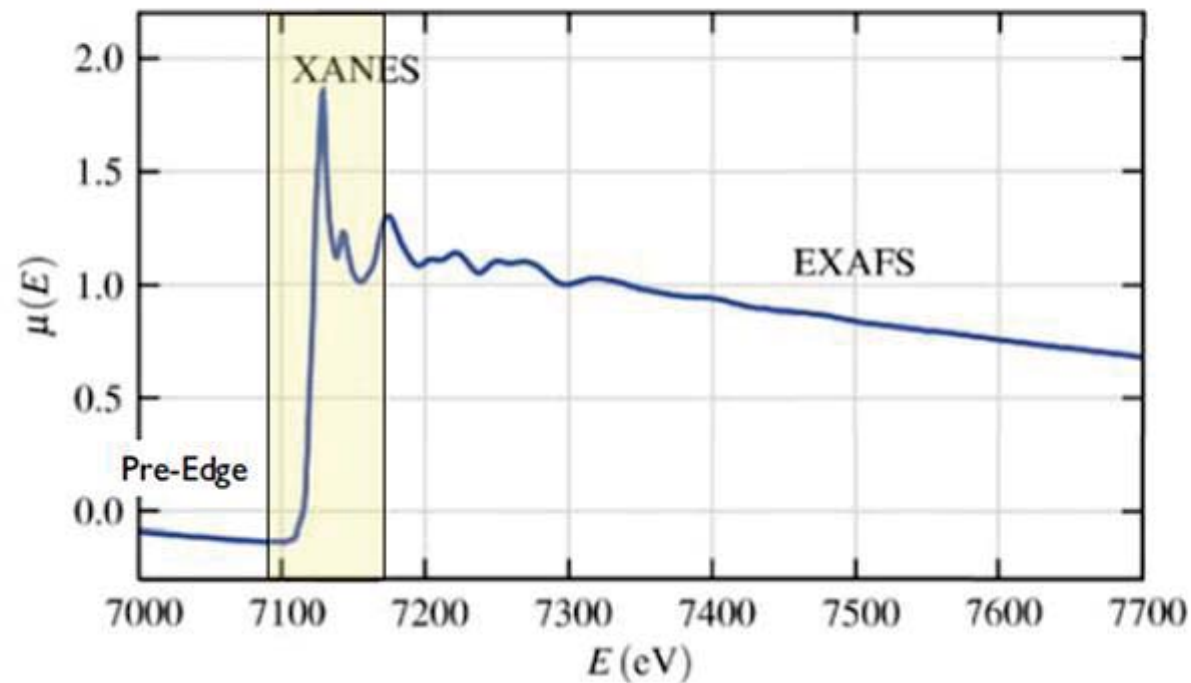
Silversmit, Anal. Chem. 2009

XAFS Characteristics

- ❖ Elemental specificity
- ❖ local atomic coordination
- ❖ chemical state
- ❖ works at low concentrations
- ❖ small sample masses (even monolayers)

XANES vs EXAFS

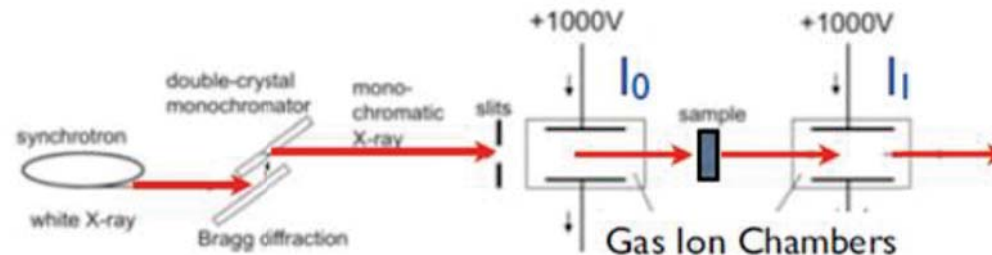
Fe *K*-edge XAFS for FeO:



XANES X-ray Absorption Near-Edge Spectroscopy (0-40 eV)

EXAFS Extended X-ray absorption Spectroscopy (40-1000 eV)

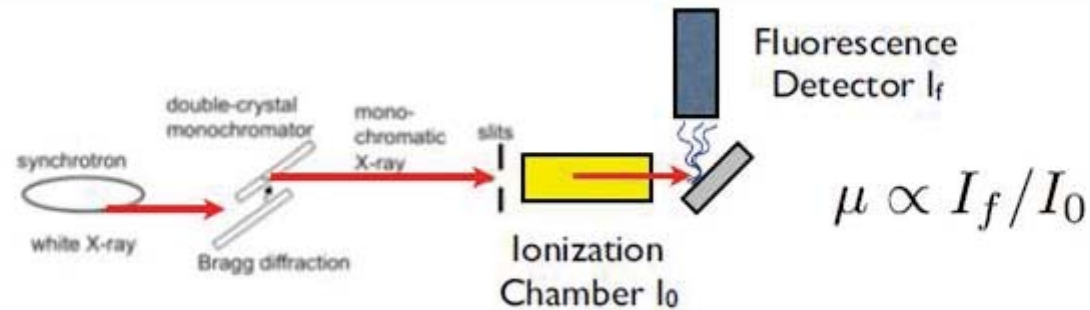
Transmission



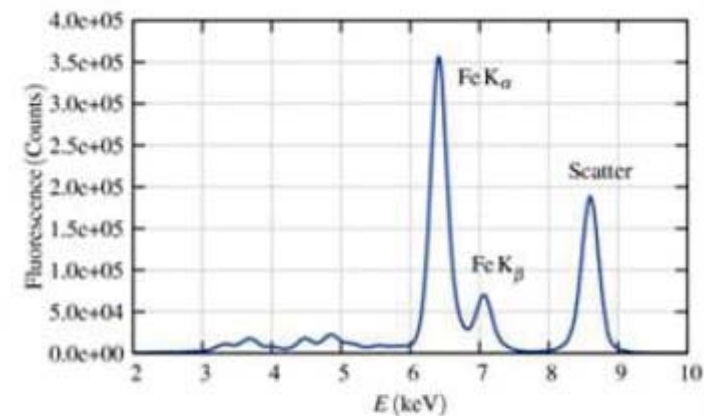
$$\mu(E)t = -\ln(I/I_0)$$

- For concentrated samples, transmission is often best technique for XAFS, but proper sample preparation is required
- Want $\mu_{\text{Above}} - \mu_{\text{Below}} = \Delta\mu \ni 1 < \Delta\mu < 3$
- For Fe foil $\Delta\mu=1$ requires 3.7 μm thick foil!
often solution is to make BN+sample powder pellet
- samples must be uniform without pinholes
- the grain size must be smaller than the absorption length

Fluorescence Measurements



- Concentrations down to the ppm level can be measured
- Background from other signals can dominate leading to dead time poor S/N
- Sample non-uniformity big problem (I_0 correction can fail)



X-ray Fluorescence Spectrum

Radioactive „hot” particles:

Localised aggregates of radioactive atoms resulting in inhomogeneous distribution of radionuclides significantly different from that of the matrix

Sources of radioactive particles dispersed in the environment

Nuclear fuel cycle, former authorised emissions

Nuclear weapons test sites: (Nevada, US; Maralinga, Australia; Mururoa, French Polynesia; Semipalatinsk, Kazakhstan plutonium concentrations in excess of $100,000 \text{ Bq kg}^{-1}$ dry soil);

Areas contaminated by crashed reactor powered satellites (Cosmos 954, Canada);

Aircraft carrying nuclear weapons (Thule, Greenland, Palomares, Spain)

Characterisation of Radioactive Particles

- **Bulk methods:** α -, γ -spectroscopy, XRF
- **Nuclear tracks:** α -tracks, β -autoradiography, fission tracks
- *hot spots related to particles: sub-samples collection.*
- **SEM-EDX:** morphology, dimension, elemental composition of minor elements;
- **micro-XRS** trace analysis of selected particles
- **SIMS:** isotopic ratios, morphology, depth profile, Imaging (3D) and elemental composition.

Comparison of microanalytical techniques for analysis of hot particles

<i>Technique</i>	<i>Projectile/ Quantum energy (keV)</i>	<i>Beam Size (μm)</i>	<i>Beam Penetration (μm)</i>	<i>Minimum Detection Limit (ppm)</i>	<i>Destructive</i>	<i>Calibration</i>
EPMA	e^- , 5-50	<0,1	1-10	1000	no	easy
μ-PIXE	P^+ , $2\text{-}3 \cdot 10^3$	0,3-5	5-100	1-100	yes/no	easy
μ-SRXRF	X, 2-80	0,7-10	100-1000	0,1-100	no	easy
SIMS	M^+ , N^- , 10-30	0,5-10	<0,1	<1	yes	difficult
LAMMA ICP	photon	20	10	0,5-5	yes	intermediate

LLD for selected radionuclides

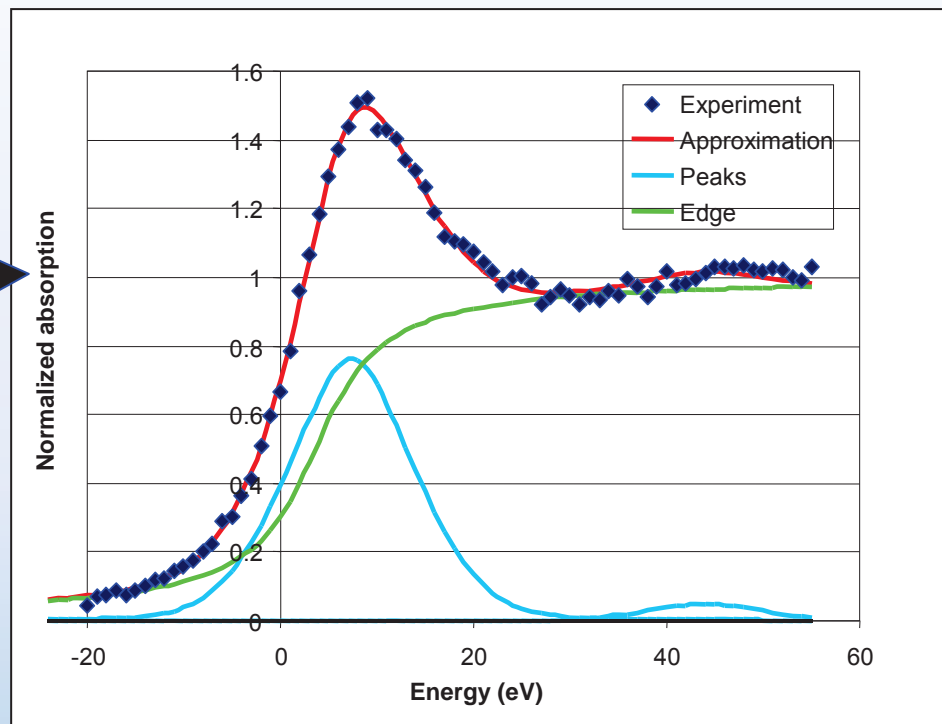
<i>Isotope</i>	<i>Sample media</i>	<i>LLD (mBq)*</i>	<i>Total content sample (fg)</i>	<i>nuclide in Method</i>
Pu-239	Soil (1 kg dry wt)	4	10	Alpha spectrometry
Pu-240	Biota (1 kg wet wt)	0.4	0.25	Alpha spectrometry
Pu-240	Air (300 m ³)	7	4.2 (10 ag/m ³)	Alpha spectrometry

*Source: Radiation risk assessment guidance (EPA, 1991)

KOSVO MICRO-XANES MEASUREMENTS OF SAMPLES

Least-square fitting of the
particle spectra

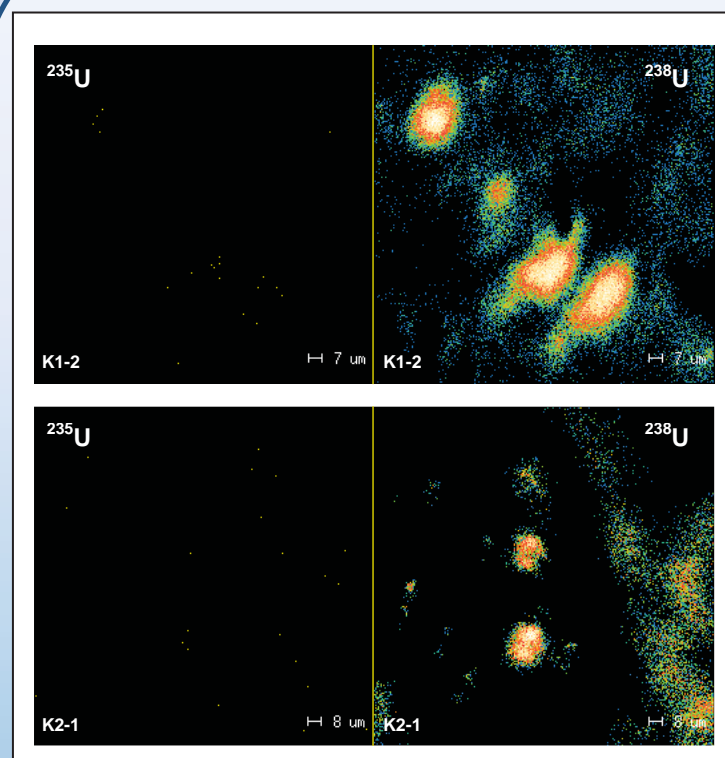
Results of least squares fitting
of the U-L_{III} XANES spectra
of six individual soil particles



	U(IV) (%)	U(VI) (%)	$I_{w(IV)}$	$I_{w(VI)}$	s_w (eV)	$I_{s(IV)}$	$I_{s(VI)}$	s_s (eV)	RMS error
K 1a	100	0	0.887	0.000	7.789	0.081	0.000	19.560	0.029
K 1b	79	21	0.817	0.222	6.323	0.115	0.158	6.068	0.023
K 4a	100	0	0.763	0.000	6.882	0.048	0.000	5.967	0.019
K 4b	90	10	0.711	0.081	6.363	0.038	0.022	4.656	0.025
K 4c	92	8	0.736	0.065	6.801	0.072	0.031	5.370	0.031
K 4d	77	23	0.663	0.200	6.015	0.078	0.121	5.249	0.030

Measured at
Hasylab

CHEMICAL AND MORPHOLOGICAL CHARACTERISATION OF KOSOVO PARTICLES

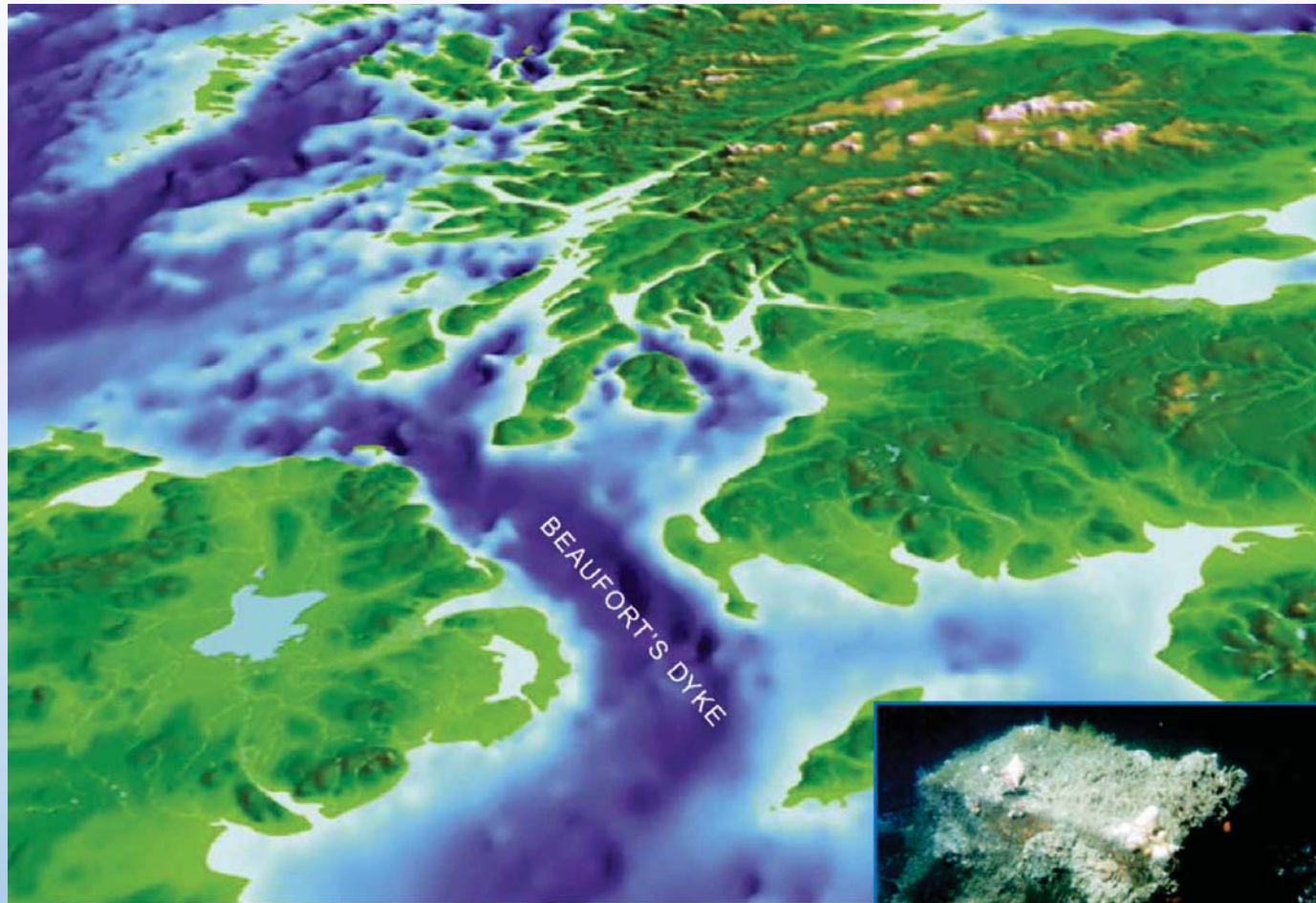


Particle	^{234}U		^{235}U		^{236}U		^{238}U	
	N°	wt %	1σ	wt %	1σ	wt %	1σ	wt %
1		0.004	0.001	0.215	0.021	0.004	0.002	99.778
2		0.005	0.003	0.207	0.021	0.003	0.001	99.785
3		0.003	0.003	0.214	0.031	0.007	0.004	99.775
4		0.001	0.001	0.207	0.014	0.003	0.002	99.789
5		0.001	0.000	0.194	0.010	0.003	0.001	99.802
6		0.001	0.001	0.196	0.013	0.003	0.001	99.800
7		0.001	0.000	0.202	0.011	0.004	0.001	99.794
8		0.000	—	0.210	0.017	0.003	0.002	99.787
9		0.001	0.000	0.196	0.006	0.003	0.000	99.800
10		0.001	0.001	0.195	0.005	0.004	0.002	99.799
11		0.000	0.001	0.201	0.013	0.002	0.002	99.796
12		0.001	0.001	0.202	0.010	0.003	0.002	99.794
Average		0.002		0.203		0.003		99.792

SIMS image

Isotopic composition of individual particles

MARINE CONTAMINATION IN THE VICINITY OF SELLAFIELD



Munitions case.

Anthropogenic radioactivity in the Irish marine environment

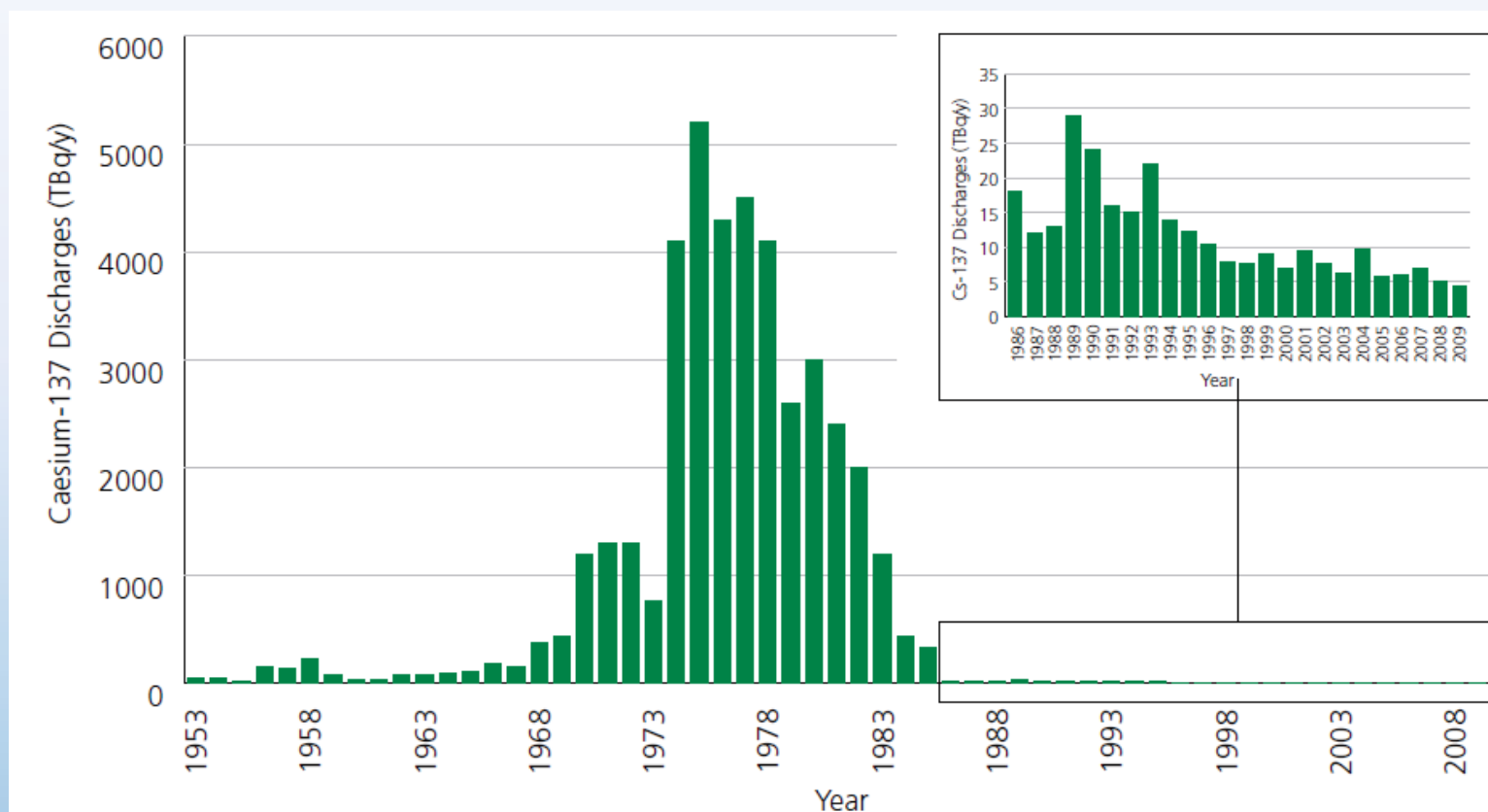
Sellafield



Radionuclides	Discharges (TBq)
Tritium	1510
Carbon-14	8.19
Technetium-99	3.08
Caesium-134	0.141
Caesium-137	4.27
Plutonium (alpha)	0.120
Americium-241	0.0463

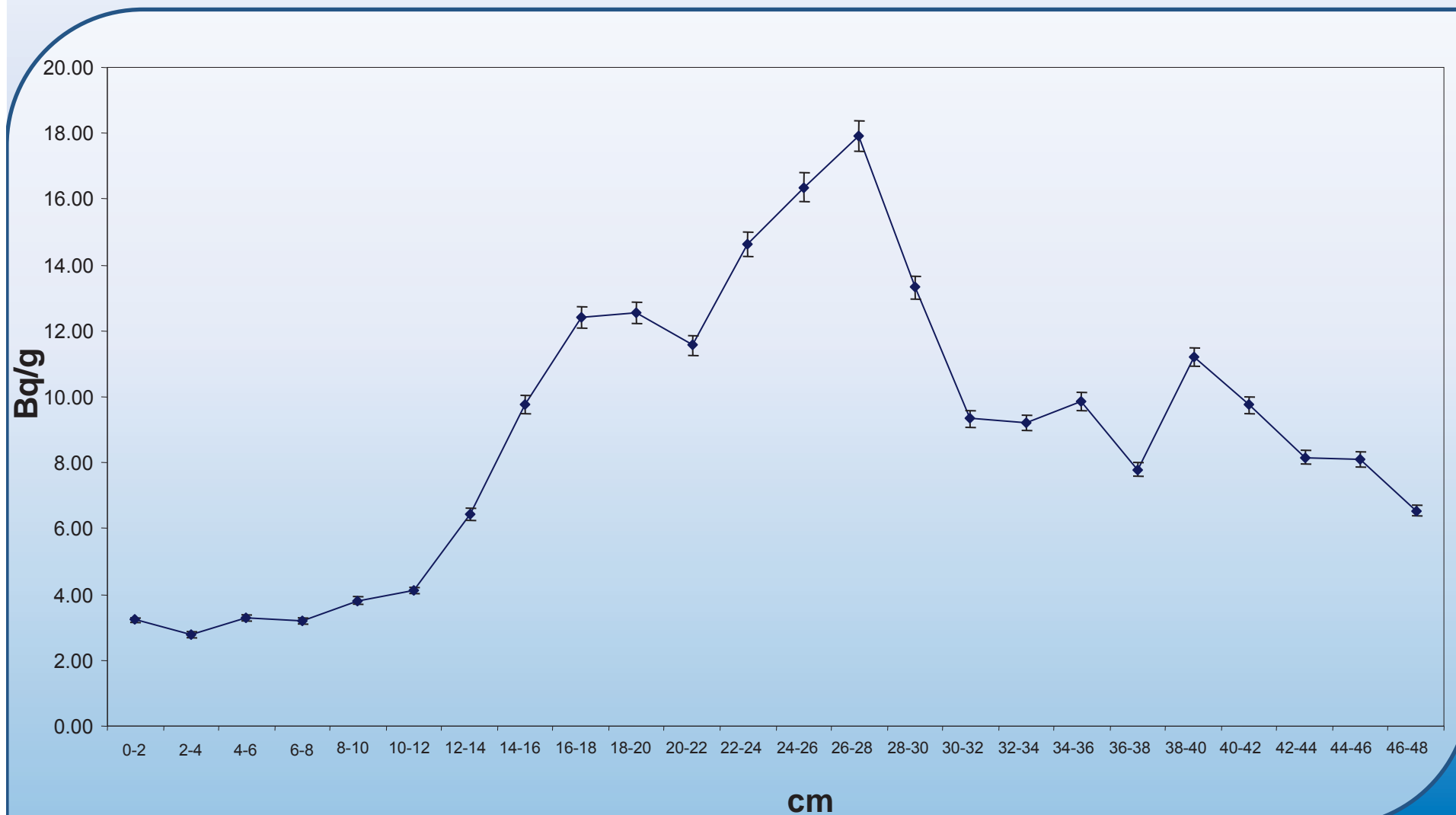
2009 Liquid discharges

Anthropogenic radioactivity in the Irish marine environment

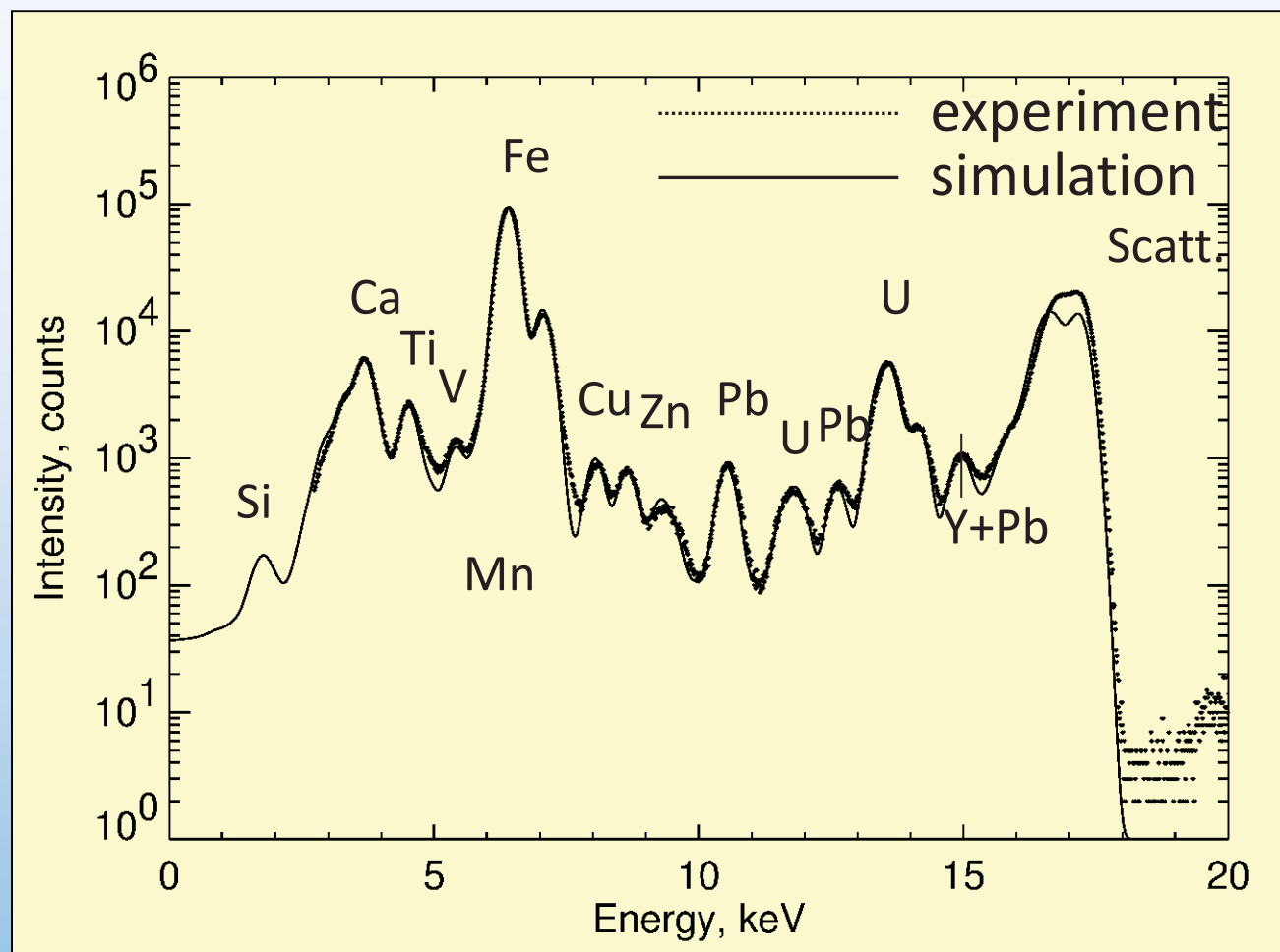


Marine discharges of caesium-137 from Sellafield, 1953-2009

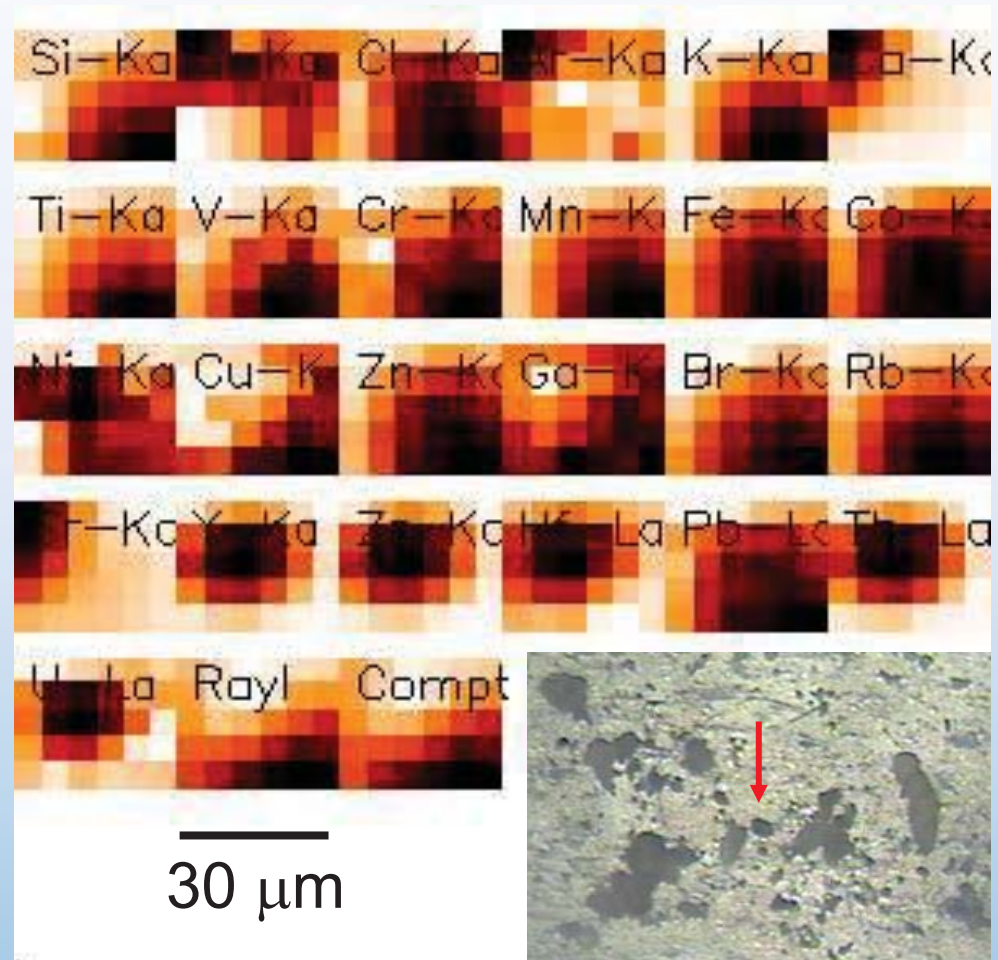
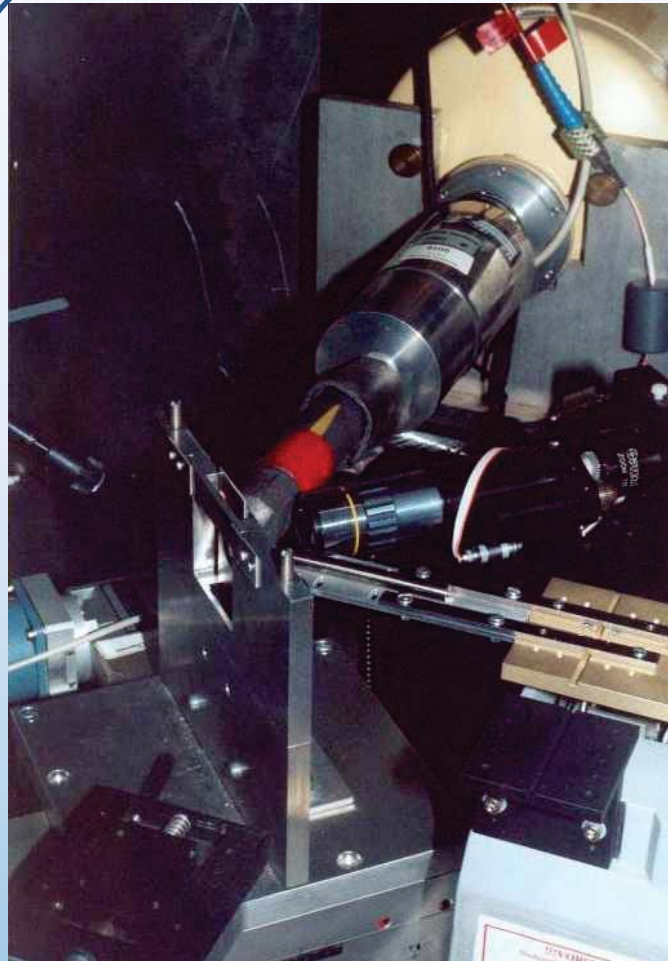
Irish Sea sediment core 241Am



COMPARISON OF EXPERIMENTAL AND SIMULATED XRF SPECTRA FROM A KOSOVO PARTICLE OBTAINED AT HASYLAB BEAM LINE L



μ -XRF measurements at HASYLAB



Sellafield sediment particle X-ray maps (U-content: 20 ppm)
Similar distribution for Zr, Hf, Th, U

Pu rich particle in
sediment around Thule
accident

Measured at ANKA

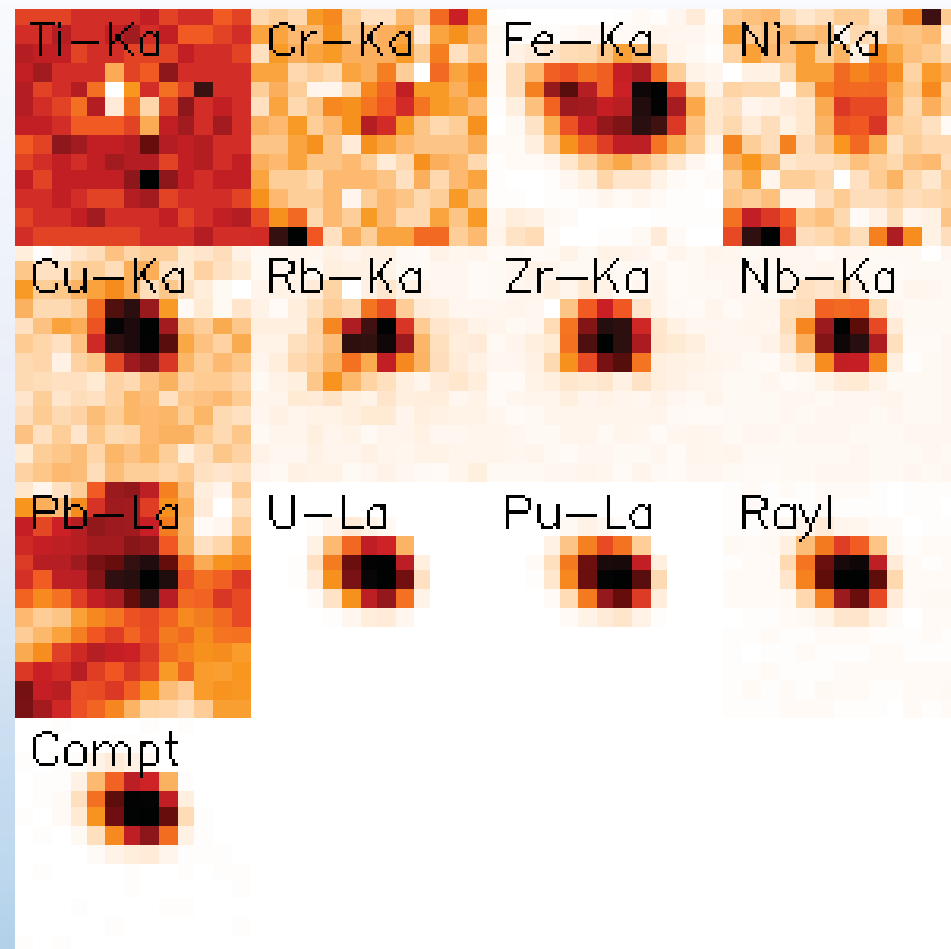
multilayer
monochromator 23 keV

beam size 20 μm

Pu major component

Pu/U 1/3

weapon grade



Micro-XRF tomography

3D elemeloszlás Fe Sr U Pu
Thule Mururoa

ANKA FLUO

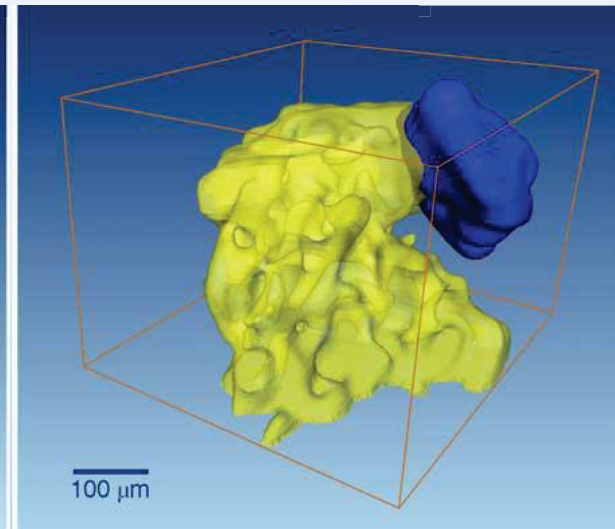
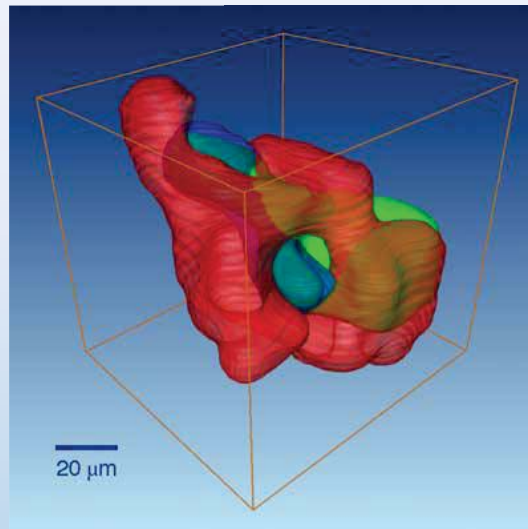
$E_0=21\text{ keV}$, $\Delta E/E=0.02$

Rotation: 0-360°, 6° steps

Beam size:

Thule: 11 μm

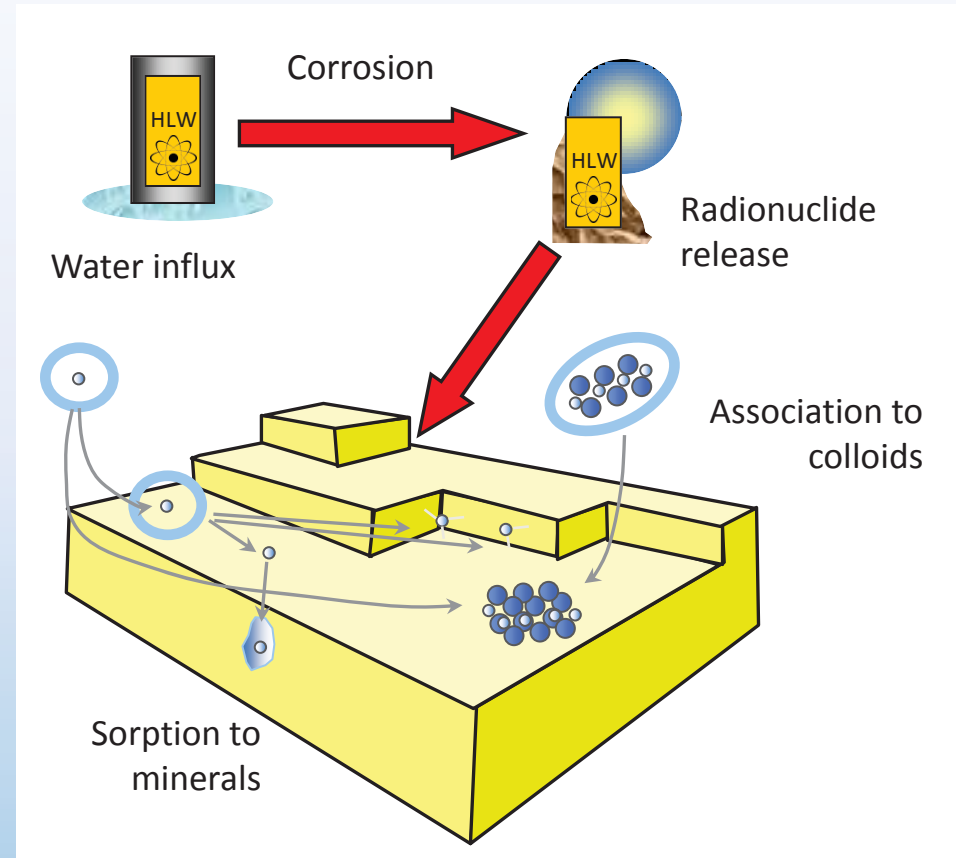
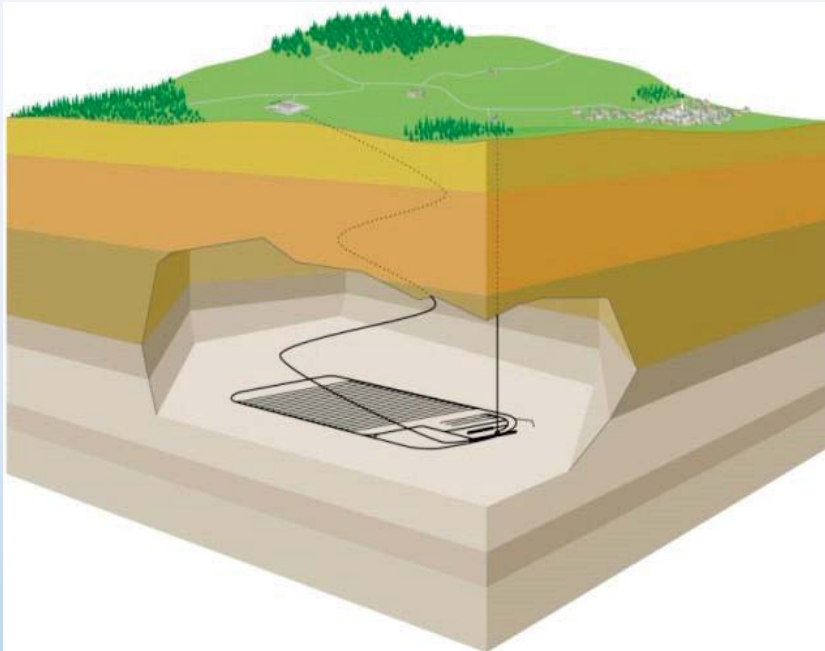
Mururoa: 19 μm



200 μm

Eriksson M, Osán J, Jernström J, Wegrzynek D, Simon R, Chinea-Cano E, et al.
Spectrochim. Acta B 2005, 60, 455-469

Radionuclide release in a nuclear repository



Size scale

Geology (1000 m)

Geochemistry (0.0000000001 m)

Time scale

Reactions (0.0000000001 years)

Half lives (1000000 years)



Optical microscopy

X-ray diffraction and XRF

Autoradiography

SR XRF, XRD, XANES

EFAFS ($>3\mu\text{m}$)

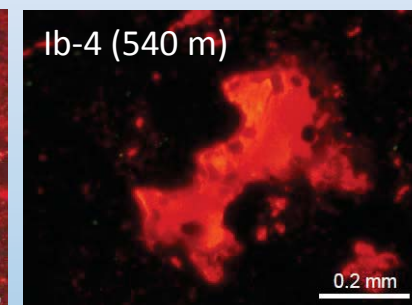
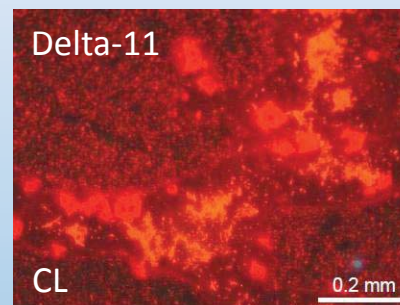
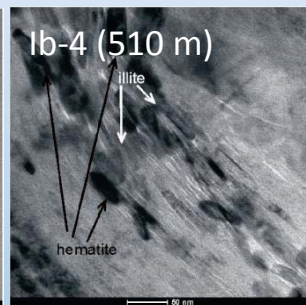
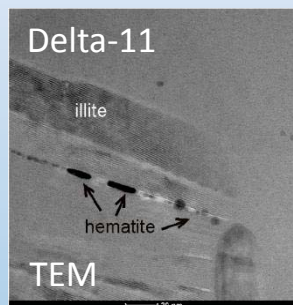
SEM TEM



Mineralogical and geochemical characterization of BCF

	10 Å	Chlorite	Analcime	Quartz	Albite	Calcite	Dolomite	Hematite
Ib-4 (510 m)	71	2		6	5	9	1	4
Ib-4 (540 m)	51	1	13		12	16		9
Delta-11	36	2		4	35	6	6	13

- Powder XRD: No significant (< 10 %) swelling clay content;
- 10-20 % interstratified chlorite/smectite with 50 % swelling component in the sample Ib-4 (540 m).

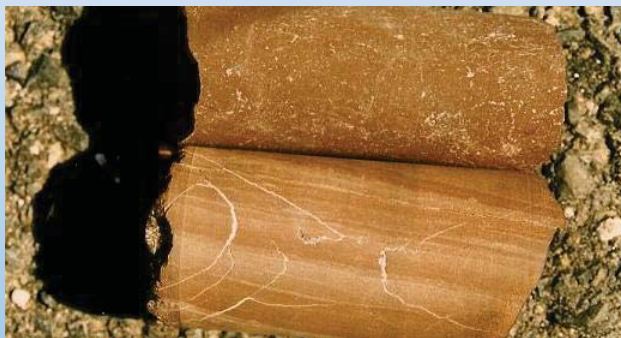


- Transmission Electron Microscopy: very small hematite flakes between illite plates
- Cathodoluminescence: Delta-11 two generations of calcite and dolomite; Ib-4 one generation of calcite

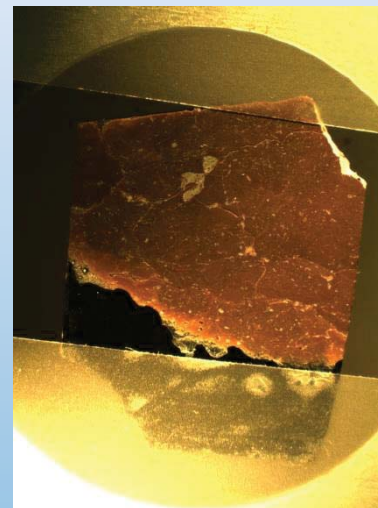
Sample preparation

Thin sections:

- polished thin sections (ca. 40 μm) on Si wafers prepared from West Mecsek Anticline (Delta-11) and Gorica Block (Ib-4) cores
- thin sections prepared on in order to keep the rock intact
- preparation of 350 μm thick Si wafers allowing transmission mode micro-XRD measurements
- 72-h sorption experiments using 0.1 M NaCl as background electrolyte, concentration of added Cs(I), Ni(II), Nd(III), or U(VI) estimated using sorption modelling (10^{-6} – 10^{-3} M depending on element)



Drilled core



Thin section
On Si backing
In sample
holder

Measurement methods

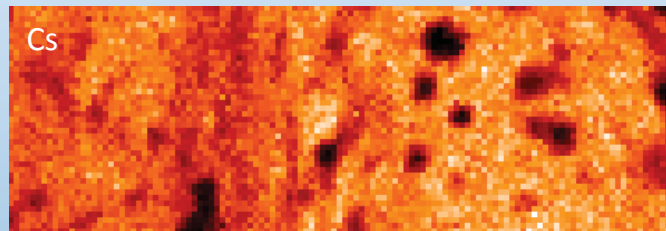
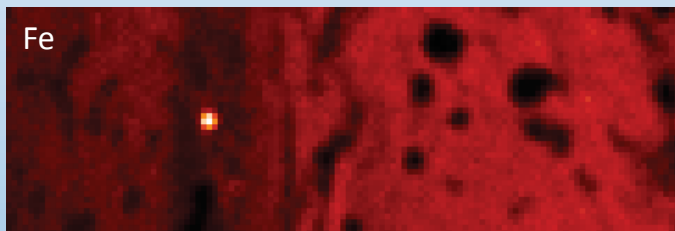
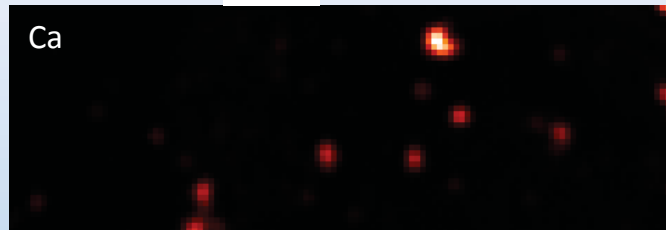
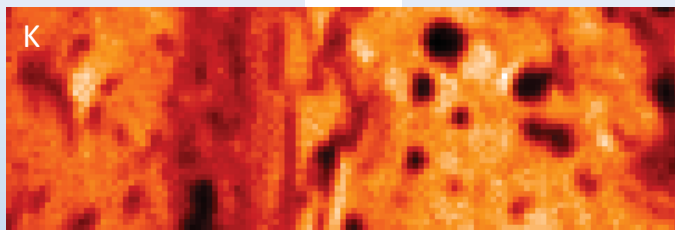
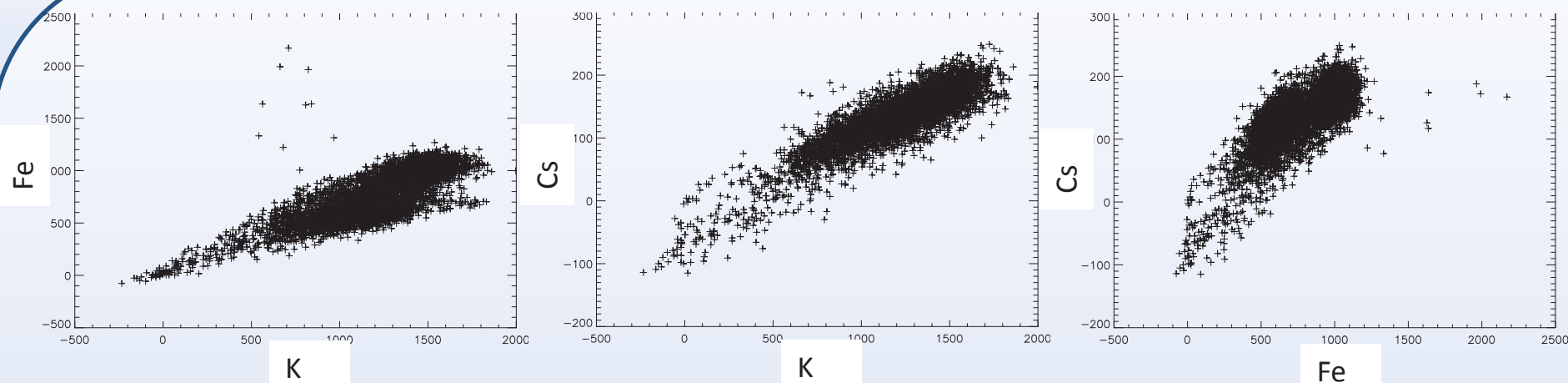
Laboratory:

- (LV)SEM/EDX
- laboratory-scale micro-XRF at 50 μm resolution
 - pre-selection of areas of interest

Synchrotron radiation methods:

- HASYLAB Beamline L (Hamburg, Germany): combined μ -XRF/XRD/EXAFS at 20 μm resolution
- ANKA FLUO Beamline (Karlsruhe, Germany): combined μ -XRF/XRD at 5 μm resolution
- μ -XRF scanning mode: 2D distribution of elements
 - inter-elemental correlations
 - multivariate statistical methods
 - basis for selecting positions for further investigations
- μ -XRD: crystalline phase composition at selected positions
- (μ -XAS: local environment and valence state of the element of interest)

Samples treated with Cs(I) solution

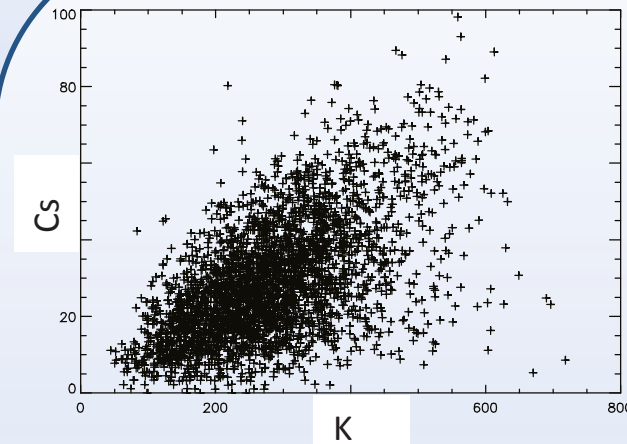


IB4 sample
treated with
0.36 mM Cs⁺

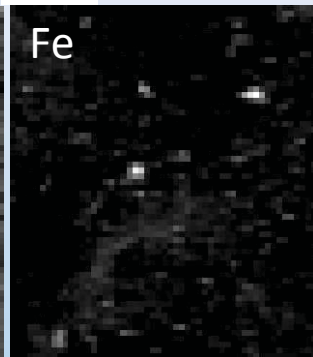
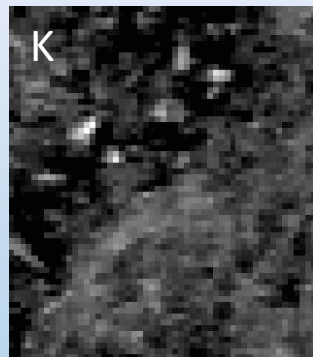
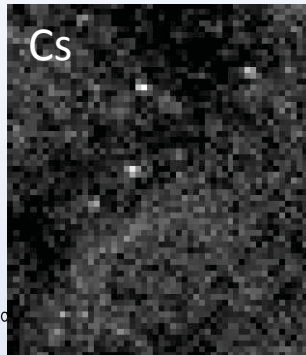
Elemental maps laboratory micro-XRF (EK) 1x4 mm² area,
40 μm stepsize (Cr anode X-ray tube, monocapillary optics)



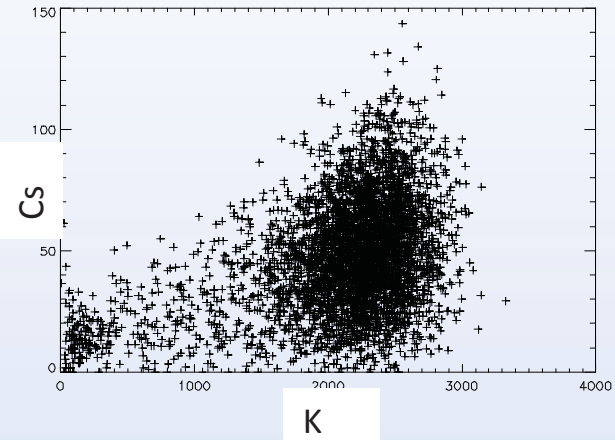
Samples treated with Cs(I) solution



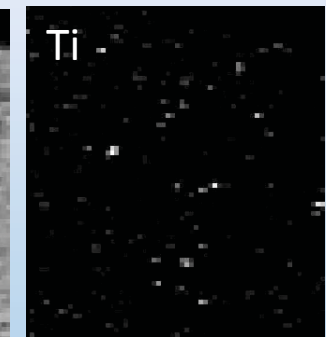
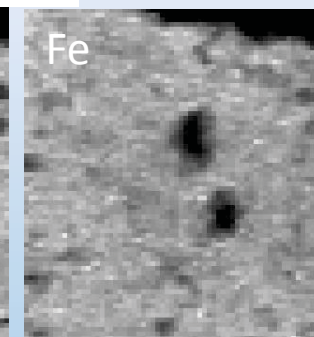
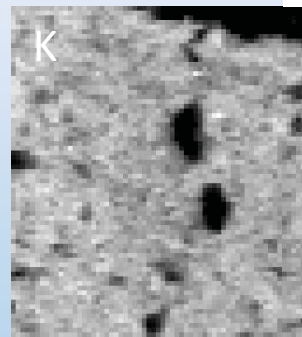
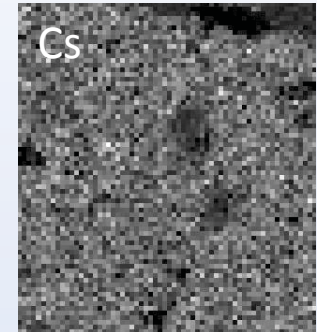
IB4



0.35×0.3 mm²



D11



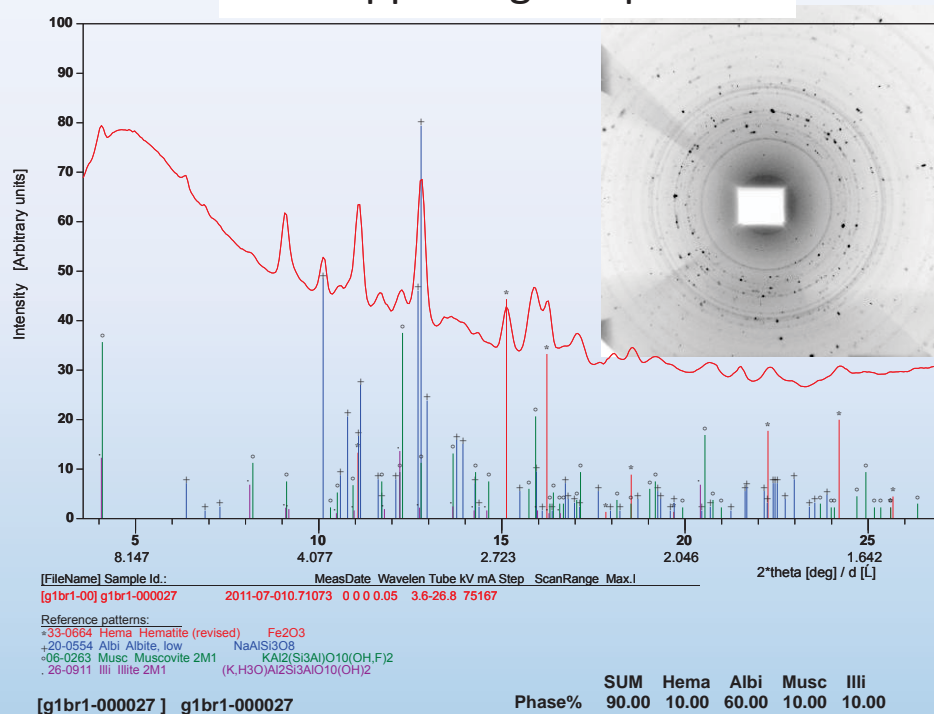
0.3×0.21 mm²

Measurement: ANKA Fluo, Karlsruhe

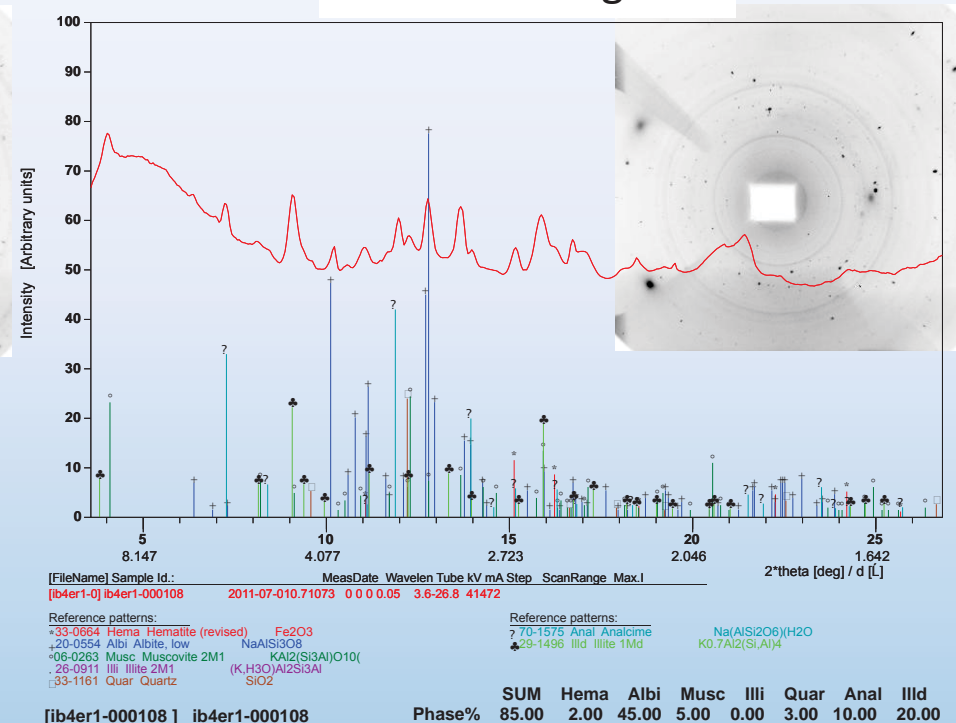
$E_0 = 17.5$ keV, 5 μ m stepsize

2D XRD images and results of azimuthal integration

Self supporting sample

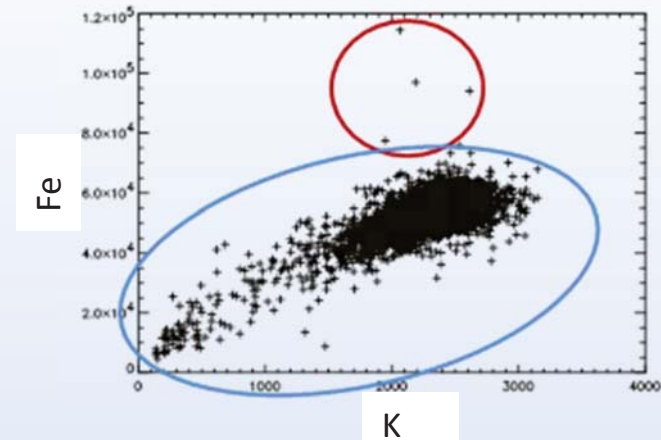
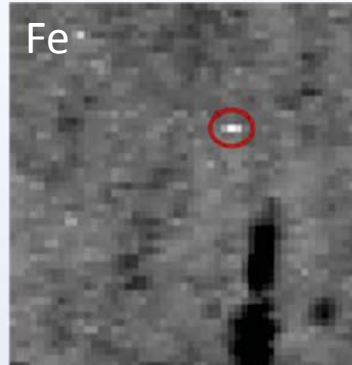
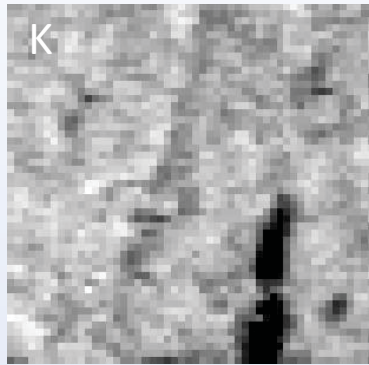


Si backing

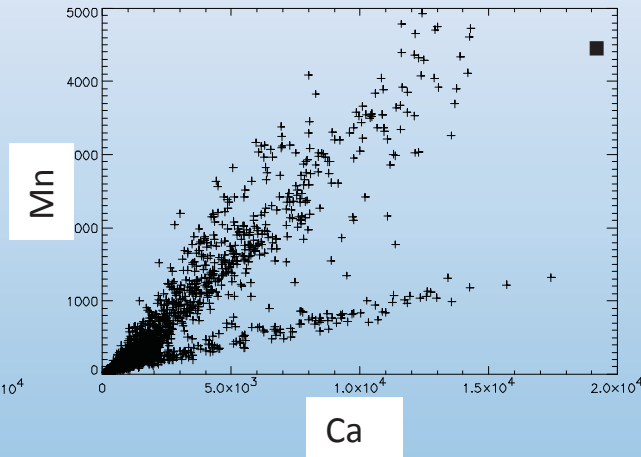
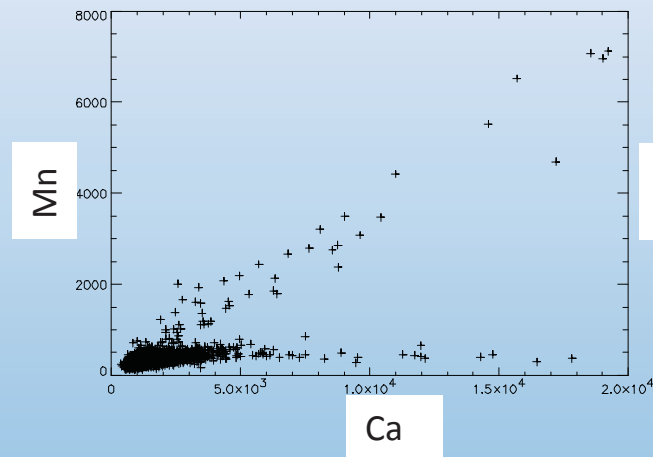


- Diffraction rings related to clay minerals are clearly visible using Si backing.
- Analyses with 5 μm beam diameter: oriented microcrystals can affect quantification
- measurement: ANKA FLUO

Micro-XRF – inter-elemental correlations



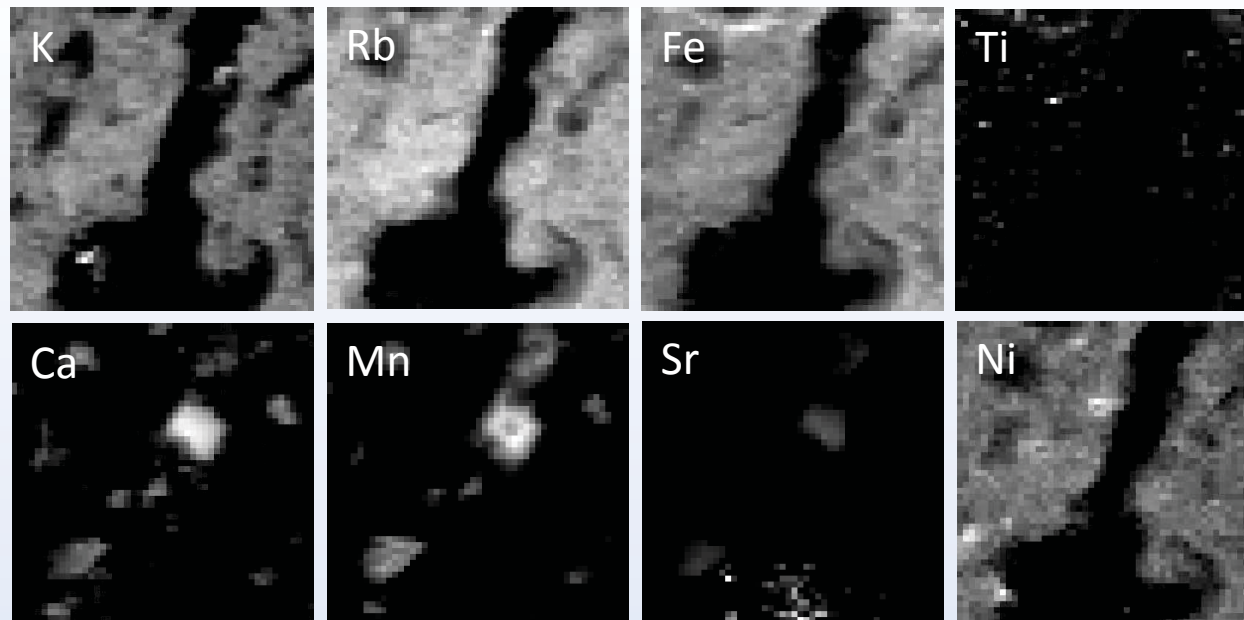
- K-Fe correlation: clayey matrix (Fe content of illite + nanocrystalline hematite)
- Outliers: Hematite, K feldspar



■ Ca-Mn correlation:
different carbonate
minerals

D11

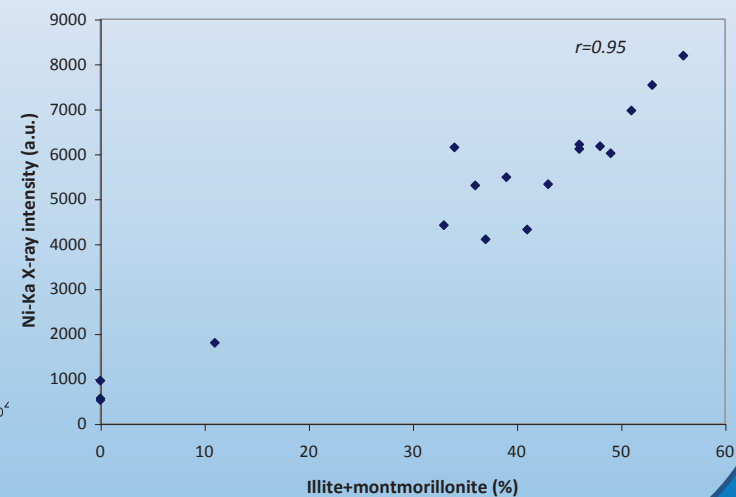
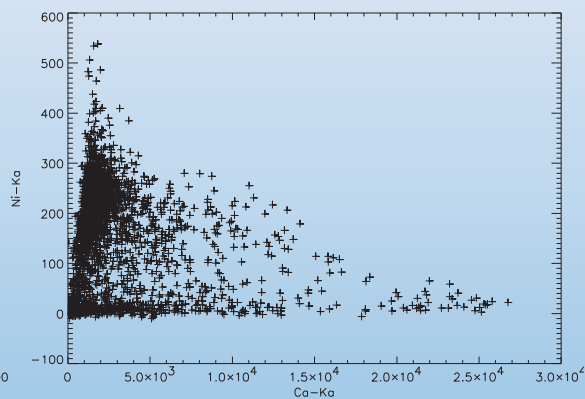
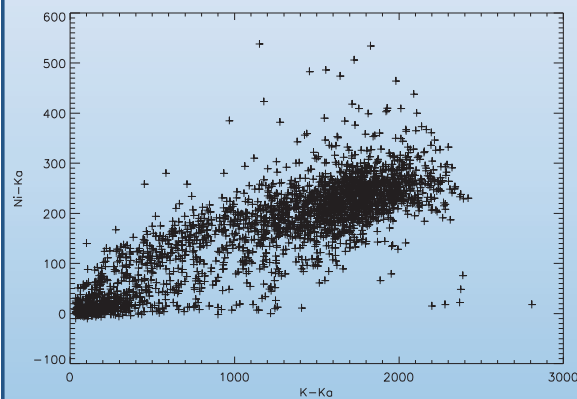
treated with
Ni(II)
solution



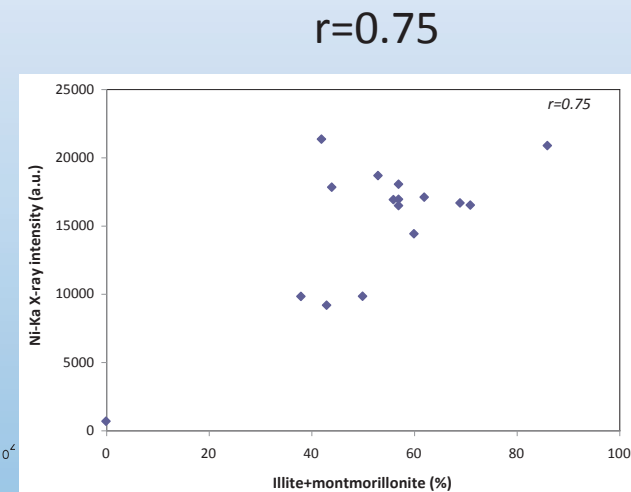
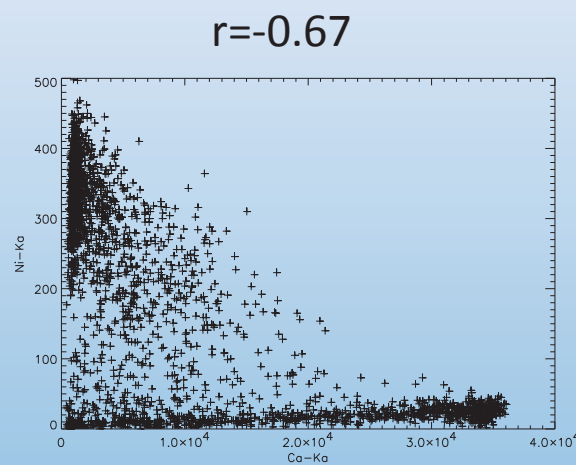
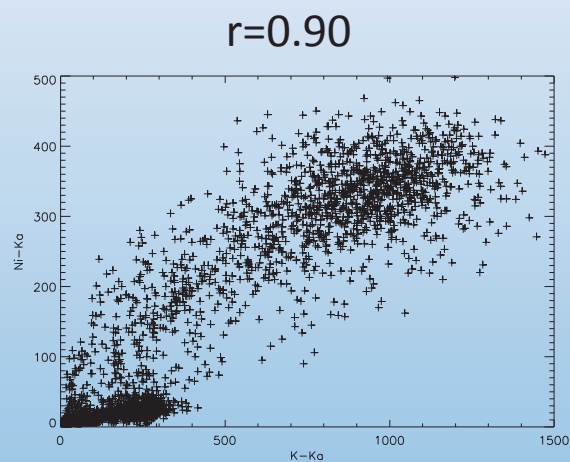
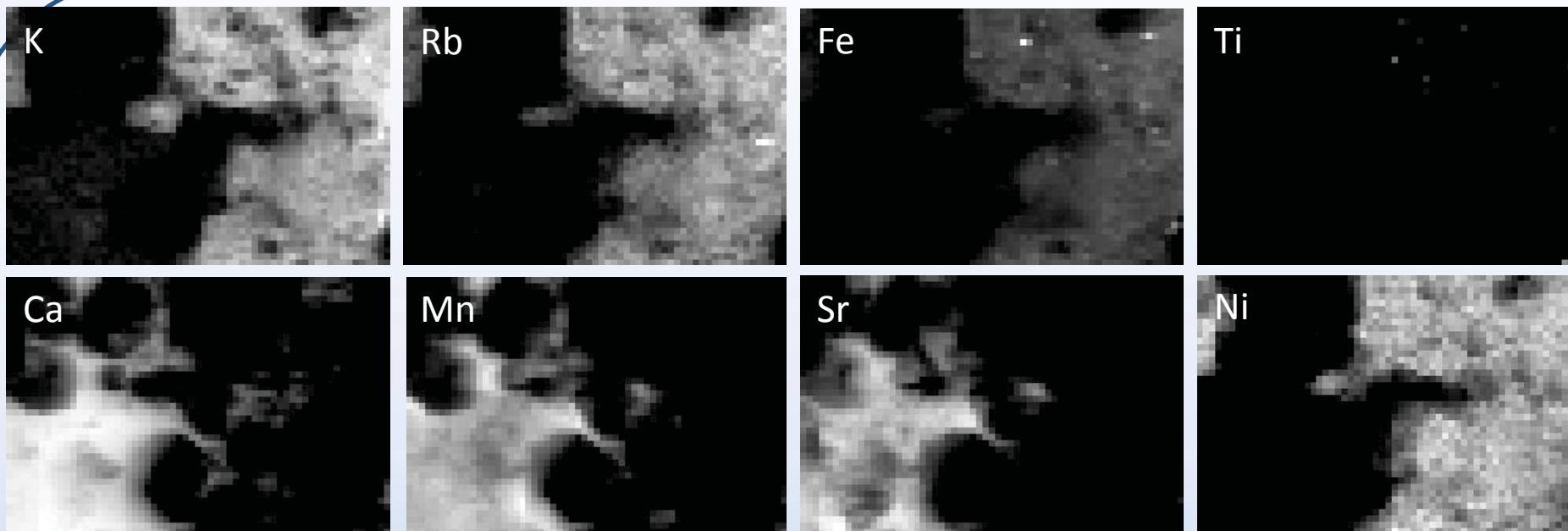
$r=0.85$

$r=-0.25$

$r=0.95$



IB4 treated with Ni(II) solution



Summary

- Instrumental development is faster than research request
- Special beam line parameters can be selected to be optimal for applications
- No need to use radioactive isotopes
- Sensitivity comparable with present nuclear spectroscopy tools
- Large data sets in one experiment, strategy is needed for efficient beam time use